UCRL-93297
PREPRINT

MATERIAL EVALUATION USING OPEN-ENDED RESONATORS

R. J. King
V. R. Latorre

This paper was prepared for submittal to
NDT Handbook on Electromagnetic Tests

August 1985

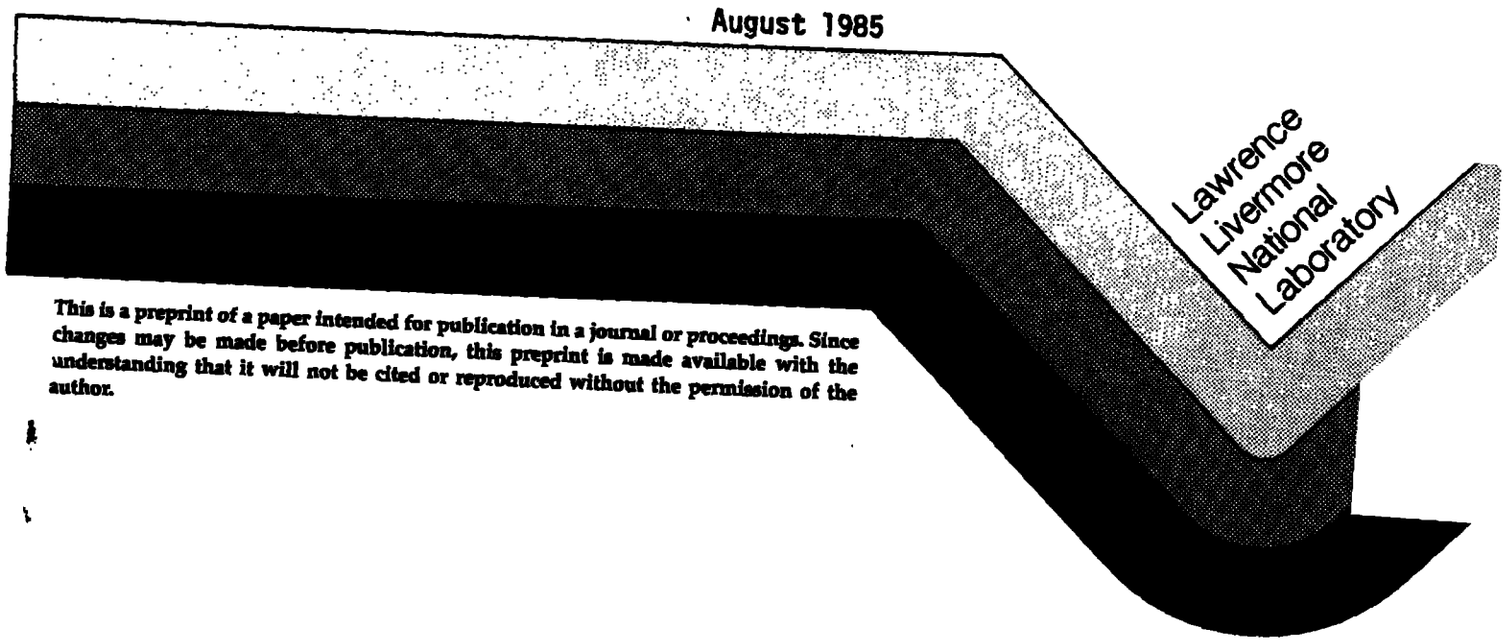

MATERIAL EVALUATION USING OPEN-ENDED RESONATORS*

R. J. King and V. R. Latorre
Lawrence Livermore National Laboratory
Livermore, CA 94550

1. INTRODUCTION

The overwhelming majority of microwave techniques for measuring the bulk properties of materials are based either on transmission through or reflection from the test medium. Moreover, these techniques are usually based on absorption of the microwaves and few use phase measurements to monitor the properties of materials. As moisture has strong absorptive properties at the higher microwave frequencies (> 2 GHz), these techniques are useful for quantifying moisture contents which are a few percent or higher. Instruments which are sensitive to the phase of the microwave signals are lacking, as are also instruments for measuring low moisture contents in solids.

In most transmission and reflection techniques, the volume of material being tested is generally of the order of many tens of cubic centimeters. There are, however, many applications where the local bulk properties of the test medium are desired in volumes of a few cubic centimeters or less. For example, such instruments are useful for mapping the *in situ* spacial variations of moisture or density of advanced composites. More specifically, these quantities are characterized by the local bulk *dielectric* properties of the material. In turn, the dielectric properties are strongly influenced by the presence of moisture, porosity, delaminations, cracks, and broken fibers,

* Work performed under the auspices of the U.S. Department of Energy by the Lawrence Livermore National Laboratory under contract number W-7405-ENG-48.

by the composition, including fiber/filler ratio [1] and the presence of foreign matter, and by the degree of cure and aging [2,3].

In contrast to absorption effects, such instruments must operate on the principle of phase measurement, or equivalently, on the dielectric properties of the test material. Consequently, they function best when testing materials having a small loss tangent ($\tan \delta < 0.1$). This generally excludes graphite type composites or materials having moisture contents greater than a few percent.

To achieve small spacial resolution for mapping purposes and sufficient sensitivity to small changes in the bulk dielectric properties, the microwaves can be coupled to the test medium via a contacting open-ended coaxial resonator [1-4]. The response of the resonator to swept frequency excitation can be sensed using coherent detection techniques [2,3,5,6]. The following describes such an instrument and gives results of its performance.

2. THE OPEN-ENDED COAXIAL RESONATOR COUPLING DEVICE

The coupling device (sensor) can have a variety of forms, but must be small enough to achieve the desired spacial resolution. A rigid open-ended coaxial line which can be placed against material has been found to be most useful [1-4] (Fig. 1). The evanescent fringing fields at the end of the sensor penetrate the material being tested so as to effect the reflection coefficient at its end, Γ_L. Thus, the test material represents an effective admittance $Y_L = G_e + j\omega C_e$ where C_e is proportional to the effective real dielectric constant ε', and G_e is the sum of the radiation conductance, G_r, and the loss conductance G_ℓ. For low loss materials, the capacitive susceptance is the dominant term in Y_L.

An analytical/numerical solution for computing the reflection coefficient of an open-ended coaxial line has been given by Mosig et al. [7], while Stuchly et al. [8,9] approach the problem more from an experimental/empirical point of view. No doubt these can be of benefit in quantifying the complex dielectric constant of materials using the resonator described here.

To ensure proper positioning of the coaxial line against the material and to provide a ground plane on which the penetrating E-field lines can terminate, a metal flange is usually provided at its end. Misalignment causes an air gap which strongly effects C_e and hence Γ_L. Although the flange in Fig. 1 is shown flat, it can be configured to fit surfaces of known curvature.

The reflection coefficient is related to the admittance by

$$\Gamma_L = \frac{Y_o - Y_L}{Y_o + Y_L} \tag{1}$$

where Y_o is the characteristic admittance of the coaxial line. While it is possible to directly measure Γ_L using an automatic network analyzer [7-9], such an instrument is costly, bulky, and not sufficiently accurate or stable to monitor minute changes in Γ_L (or ε') for most advanced composite material applications. Making the coaxial line resonant solves this problem since small changes in the argument of Γ_L causes a significant change in the resonant frequency, f_r. In turn, f_r is measurable with great precision. The quality factor, $Q(= f_r/\Delta f$, where Δf is the half power bandwidth) is another measurable parameter. In effect, the resonator transforms the observable quantities from Γ_L (amplitude and argument) to f_r and Q.

The great sensitivity of f_r to small changes in ϵ' (or argument of Γ_L) is a key feature which is best understood by analyzing the response at the resonator input. Resonance, of course, is due to the cumulative interference of multiple waves bouncing between the two ends of the resonator. If the reflection coefficients as seen by the coaxial line at its input and output are Γ_s and Γ_L, respectively (Fig. 1), then the total reflected wave traveling toward the left just inside the left end of the resonator is

$$\overleftarrow{b}_{resonator} = b_s \frac{\Gamma_L e^{-j2\beta\ell}}{1 - \Gamma_s\Gamma_L e^{-j2\beta\ell}} \tag{2}$$

where b_s is the incident field launched by the input transformer (e.g., a small coupling loop) and $\beta\ell(= \omega\ell/c)$ is the electrical length of the coaxial line. For comparison, the wave traveling toward the left of a simple coaxial line (not a resonator) of equal length and incident field is

$$\overleftarrow{b}_{coax} = b_s \Gamma_L e^{-j2\beta\ell} \tag{3}$$

taking the ratio of (2) and (3),

$$\frac{\overleftarrow{b}_{resonator}}{\overleftarrow{b}_{coax}} = (1 - \Gamma_s\Gamma_L e^{-j2\beta\ell})^{-1} \tag{4}$$

Equation (4) can be considered to be the amplification factor for the response of the coaxial resonator relative to that of a coaxial line. Near resonance this factor is quite large since $\Gamma_s = -1$ and $|\Gamma_L|$ is also nearly unity.

The reflection coefficient actually measured at the feed point just outside the resonator is proportional to (2), but inverted by the coupling arrangement so that its magnitude is small at resonance and near unity far from resonance. It is zero at resonance if the resonator is critically coupled to the feed line. In practice, critical coupling can only be achieved for a given resonator coupling arrangement and termination. When the termination changes, the resonator is no longer critically coupled. Achieving near-critical coupling for a given termination is largely a cut-and-try procedure in design.

Resonance occurs when the denominator in (2) is minimum, or

$$2\beta_r \ell = 2n\pi + \arg\Gamma_s + \arg\Gamma_L \quad , \tag{5}$$

where n = 0,1,2..., representing resonance mode number. The length of the resonator is chosen according to the desired resonant frequency. Using (5) and assuming $\Gamma_s \approx e^{j\pi}$,

$$\ell = [(2n+1)\pi + \arg\Gamma_L]\ \lambda_r/4\pi \tag{6}$$

where λ_r is the wavelength in the coaxial line at resonance. According to [7], $\arg\Gamma_L$ is a small negative angle for a dielectric termination, e.g., $\Gamma_L \approx 0.9\ e^{-j30°}$ for $\varepsilon' = 8$. Thus, ℓ is slightly less than an odd multiple of $\lambda_r/4$. In the design used here, the length was chosen to be slightly less than $3\lambda_r/4$ at 6 GHz, i.e., $\ell = 3.57$ cm for air dielectric in the coaxial line.

The inside diameter of the outer conductor is usually chosen as large as feasible to achieve maximum penetration of the fringing field into the test medium, and yet maintain only a TEM mode inside the resonator. The presence of higher order modes would obviously confuse the interpretation of any observed resonances. The next lowest (undesired) order TE mode can only exist when the average circumference is greater than half of the wavelength

$$\frac{(a + D)\pi}{2} \geq \frac{\lambda}{2} \tag{7}$$

where a is the outer diameter of the inside conductor and D is the inner diameter of the outer conductor. These diameters must also be chosen to give the desired characteristic impedance,

$$Z_o = 60 \ln (D/a) \tag{8}$$

In the present design D was chosen as 7 mm. Two center conductors having diameters of a = 3.04 mm and 2 mm were fabricated to give Z_o = 50 Ω and 75 Ω, respectively. The left end of each is threaded to permit screwing into the resonator base.

Then, according to (7), the lowest TE mode which can exist inside the resonator has cutoff frequencies of 9.5 and 10.6 GHz for Z_o = 50 and 75 Ω, respectively. These are well above the nominal 6 GHz operating frequency.

Coupling to the loop can be either inductive (e.g., a loop as shown in Fig. 1) or capacitive, which is accomplished by placing a gap between the center conductors of the feed and the resonator [4]. In the results presented

here, only inductive coupling was used. Connection between the feed and the coupling loop was via a SMA connector.

3. INSTRUMENTATION

The instrumentation for measuring the wave reflected from the resonator is shown in Fig. 2. All components are state-of-the-art microwave stripline and solid state, and connected by microcoax. A leveled 40 mW swept cw source drives the system and a reflectometer bridge having a directivity of 35 dB routes the reflected wave into a phase-insensitive coherent (homodyne) detector. To accomplish coherent detection, the reflected wave is double sideband amplitude modulated at 30 kHz before mixing with a 12 dBm cw reference signal fed directly from the source. The amplitude of the reflected wave is adjusted to be at least 30 dB below the reference signal to minimize detection errors. Full details on the operation of the phase-insensitive coherent detector are given in [5]. Here it is sufficient to remark that the output amplitude of the detector at 30 kHz is proportional to $|\Gamma|$, which is the amplitude of the desired reflection coefficient at the resonator's input. It is subsequently amplified about 65 dB and bandpass filtered at 30 kHz to remove any low frequency noise introduced in the detection process and also any higher order harmonics of 30 kHz. Finally, it is envelope detected and $|\Gamma|$ is displayed on an oscilloscope vs. the swept frequency. If desired, electronics can be added for measuring f_r and Q.

Of course, much simpler instrumentation results if the microwave source is amplitude modulated and the reflected wave emerging from the reflectometer bridge is simply video detected. The advantages of the more complicated

system shown in Fig. 2 are that the sensitivity and dynamic range are enhanced by several orders of magnitude, and the detection process is linear [6]. In the present case, sensitivity is particularly important because $|\Gamma|$ is very small at resonance, especially if the resonator is nearly critically coupled. Being able to accurately measure f_r at the minimum depends on the system noise, which is quite low in the instrumentation system of Fig. 2. Moreover, linearity is also important; video detectors are square low at low levels, and therefore tend to distort the observed minimum in $|\Gamma|$ and prevent accurate measurement of Q.

For either detection method, it is important to note that although only the magnitude of Γ at the resonator input is observed (the argument of Γ is not measured), the argument of Γ_L is in effect measured since it chiefly determines f_r [see (6)]. $|\Gamma|$ is chiefly determined by $|\Gamma_L|$ and the coupling factor β', while the overall Q is chiefly determined by the loss factor $(\sigma/\omega\varepsilon')$ of the test dielectric.

4. PERFORMANCE

Figure 3 shows the typical variation of the resonant frequency and Q for an open-ended coaxial resonator vs. the real dielectric constant ε' of the terminating medium. The sensitivity to ε' and accuracy of measurement are clearly the greatest for $\varepsilon' < 5$. At higher values of ε', the instabilities of physically placing the open face of the resonator against the dielectric are too great to give consistent results. Moreover, the overall Q becomes quite low because the loss factor of the dielectric $(\sigma/\omega\varepsilon')$ decreases with increasing ε'. This also makes accurate measurement of f_r difficult because the minimum of the response is not sharply defined.

It has been suggested [4] that the reduced sensitivity of f_r for large ε' seen in Fig. 3 can be enhanced by using a stepped resonator design. In such a design, the diameter of the inside conductor is increased in steps near the feed end.

Figure 4 shows typical resonance curves for several dielectric constants. The observation here is that the coupling factor, β', between the feed line and the inductively coupled resonator is a function of ε'. In this figure, $\varepsilon' = 4$ gives the greatest coupling. The shape of each of the resonances shows that $\beta' < 1$ (if the peaks have double maxima, of which there are none, then $\beta' > 1$). The value of ε' where the coupling is greatest can be chosen by adjusting the size of the coupling loop. This suggests that probes having different β' values may be useful for testing different materials.

4.1. SENSING MOISTURE

In situ instruments for quantifying very minute levels of moisture (< one percent) in solid materials are virtually nonexistent. This problem is particularly important for composites since the presence of moisture presents severe constraints in the manufacture and repair processes, and is a diagnostic indicator of the aging and structural integrity of in-service materials. In manufacturing and repair, moisture is reported to contribute to porosity, disbonds, and subsequent delaminations [10,11].

When microwaves interact with water, there are two dominant effects. These are best explained by understanding the properties of the complex dielectric constant of water $\hat{\varepsilon}(= \varepsilon' - j\varepsilon'')$, shown in Fig. 5. The two most important things to note are:

a) The real part of the dielectric constant, ε', is large, e.g., $\varepsilon' = 73$ at 5 GHz. Thus, a trace of moisture in a host material having a much lower ε' (say $\varepsilon' = 2.5 - 5$ for composites) has a pronounced effect on the total ε' of the mixture. This is the dominant effect which can be measured by the microwave open-ended resonator.

b) The imaginary part of the dielectric constant, $\varepsilon''(= \sigma/\omega\varepsilon_o)$, rises in the microwave range, peaking at about 17 GHz. This quantity is called the loss factor, and accounts for the dielectric viscose (friction) forces. It is the primary factor contributing to dissipation or attenuation of the microwaves.

In testing for moisture in solid dielectrics which are nearly impervious, it is very difficult to condition the dielectrics so that a known quantity of moisture is distributed uniformly throughout the dielectric. The problem is basically one of being able to obtain suitable standard materials having known moisture content. Lacking such standards for quantifying the sensitivity and accuracy of the measurement system to very low moisture contents, extensive tests were made using a hygroscopic liquid (triethylamine). Such a liquid is useful for several reasons:

a) It absorbs moisture in reasonable quantities before saturating.

b) It has a low known dielectric constant ($\varepsilon' = 2.42$) which does not vary in the frequency range of the resonator (4-8 GHz).

c) It can be "dried" to zero moisture content.

d) It does not absorb a significant amount of moisture from the atmosphere over the time scale of the calibration experiment (minutes).

e) It remains isotropic and homogeneous with the addition of moisture.

f) The resonator is easily positioned in the liquid, and "lift-off" problems are avoided.

g) It is stable in a normal environment.

For testing liquids, the face of the resonator was covered with mylar film, as shown in Fig. 6, and inserted into the liquid. The results are shown in Fig. 7, where it is seen that moisture levels of the order of 50 parts per million (ppm) are distinguishable. This is a very significant result since it demonstrates the extremely high sensitivity. This sensitivity can be substantially increased even more by using a synthesized swept frequency source and improved resonator designs. However, one should keep in mind that the instrument responds to the bulk dielectric constant, i.e., the effects of small changes in ε' of the host material are also observed. Thus, if ε' of the host material increases, the change in the response will probably not be distinguishable from a small change in the moisture. Thus, it can be said that moisture levels of 50 ppm or even less are discernable with this instrument if the dielectric constant of the host material is constant.

4.2. SENSING ANOMALIES IN SOLID DIELECTRICS

As the resonant frequency is very sensitive to the bulk effective dielectric properties very near the resonator's aperture, it can also sense the presence of small anomalies such as cracks, voids, air gaps, and porosity. Figure 8 shows the shift in f_r as the resonator traverses a crack in a low loss dielectric material ($\varepsilon' = 4$). The test specimen was fabricated by cutting a solid piece in half, polishing the cut faces, and then clamping them together again. In this and subsequent figures, the response at the resonator's input has been inverted from that seen in Fig. 4. The left curve results when the resonator is far removed from the crack, and the right curve is the response when the resonator is directly over the crack. Although the crack is exceedingly thin, the shift in f_r is clearly evident.

Sensing of a deep subsurface crack which is normal to the surface is shown in Fig. 9. In this case, a 1 mm slot was cut to a depth of 0.5 inch in a 2 inch diameter and 1 inch high teflon cylinder. The resonator was placed on the flat side away from the slot. Again, the shift in f_r is clearly discernable as the resonator traverses above the slot, being greatest when directly over the slot.

Subsurface horizontal air gaps (e.g., delaminations) can also be sensed. Figure 10 shows the response for a 2 inch high teflon cylinder cut in half by a milling tool and then stacked together again. The curve marked "laminated" is the resulting response, compared to the response of the uncut cylinder marked "solid." Insertion of one and two sheets of notebook paper between the two halves tends to move the response back toward the uncut response because the paper replaces the air in the gap and has a dielectric constant of the order of that for teflon.

Finally, the resonator can also sense the presence of subsurface anomalous materials. Figure 11 shows the difference in responses when one and two inch high teflon cylinders are placed on either a metal or ferrite microwave absorbing ground plane. Although the differences are not great because of the large thickness of the teflon, they would be substantially enhanced for thinner dielectrics. These results suggest that the evanescent field does penetrate to depths which are substantially greater than the dimensions of the sensing aperture. This has obvious application in measuring dielectric thickness [4] and mapping the location of metal support members.

5. CONCLUDING REMARKS

From these examples, it can be seen that the resonator is able to sense the presence of an anomaly, but the spacial resolution is, of course, quite limited. Thus, if one observes the change in f_r, it is unclear what the anomaly is, e.g., a crack, a void, or some other unknown anomaly, or its depth, width, exact lateral position, or variations in the thickness or dielectric constant of the dielectric. Lateral scans which are orthogonal may shed some light on the extent, general shape, and composition of the anomaly. The presence of an anomaly containing air always causes f_r to increase. Conversely, a decrease in f_r would indicate the presence of an anomaly having a larger ε' than that of the host material, e.g., moisture.

The instrument is exceedingly sensitive to small changes in the bulk dielectric properties. Its use appears very promising in quantifying the presence of moisture, porosity, density, aging and composition, and various anomalies such as cracks, voids, delaminations, broken fibers, thickness variations, foreign matter, and support members.

Considerably more research and development is needed to reduce this technology to practical field use.

REFERENCES

[1] B. Forssell, "Nondestructive Measurements of the Glass/Fiber Content in Reinforced Plastics by Means of Microwaves," 4th European Microwave Conf. Proc., September 1974, pp. 132-136.

[2] V. R. Latorre and R. J. King, "In Situ Microwave Measurements of Dielectric Properties and Moisture Measurement in Materials," Proc. of the 1985 International Moisture and Humidity Symposium, Washington, DC, April 15-18, 1985, Instrument Society of America ISBN 0-87664-865-0.

[3] R. J. King and P. Stiles, "Microwave Nondestructive Evaluation of Composites," Rev. of Progress in Quantitative NDE Conference, D. O. Thompson and D. F. Chementi, Eds., Plenum Press, New York, 1984, pp. 1073-1081.

[4] H. Moschüring, "Inhomogeneous Open-Ended Resonators as Microwave Sensor Elements," Proc. 1984 IEEE International Symposium on Microwave Theory and Techniques, May 30 - June 1, 1984, San Francisco. ISSN 0149-645X, IEEE Cat. No. 84CH2034-7.

[5] R. J. King, "Error Analysis of Phase-Insensitive Coherent (Homodyne) Detectors," IEEE Trans. on Instrumentation and Measurement, IM-31(3), September 1982, pp. 212-214.

[6] R. J. King, Microwave Homodyne Systems, Peregrinus Press, London, 1978.

[7] J. R. Mosig, J. E. Besson, M. Gex-Fabry, and P. E. Gardiol, "Reflection of an Open-Ended Coaxial Line and Application to Nondestructive Measurement of Materials," IEEE Trans. IM-30(1), March 1981, pp. 46-51.

[8] M. A. Stuchly and S. S. Stuchly, "Coaxial Line Reflection Methods for Measuring Dielectric Properties of Biological Substances at Radio and Microwave Frequencies - A Review," IEEE Trans. IM-29(3), September 1980, pp. 176-182.

[9] M. A. Stuchly, M. M. Brady, S. S. Stuchly, and G. Gajda, "Equivalent Circuit of an Open-Ended Coaxial Line in a Lossy Dielectric," IEEE Trans. IM-32(2), June 1982, pp. 116-119.

[10] Y. Bar Cohen, M. Meron, and O. Ishai, "Nondestructive Evaluation of Hygrothermal Effects on Fiber-Reinforced Plastic Laminates," J. of Testing and Evaluation, 1979, pp. 291-296.

[11] K. G. Reimer, "The Effect of Prebonding Humidity Exposure on Structural Adhesive for Advanced Composite Bonding," Lear Fan Corp. Engineering Report R43204 (Part I), December 1981, and Report R43209 (Part II), January 1983.

FIGURE CAPTIONS

Figure 1. Inductively coupled open-ended coaxial resonator is placed against the test material.

Figure 2. Coherent detection is used to measure the reflection coefficient, $|\Gamma|$, at the input of an open-ended coaxial resonator.

Figure 3. Typical variation of f_r and Q of an inductively coupled open-ended coaxial resonator vs. the real dielectric constant, ε', of the terminating medium.

Figure 4. Typical open-ended resonator reflection coefficients vs. frequency for various dielectric constants.

Figure 5. Complex dielectric constant ($\hat{\varepsilon} = \varepsilon' - j\varepsilon''$) of free water vs. frequency.

Figure 6. The open-ended resonator can be used to measure the dielectric properties of liquids.

Figure 7. Resonant frequency vs. water content in triethylamine.
ppm → parts per million

Figure 8. Typical shift in response when an open-ended resonator passes over a deep crack in a dielectric.

Figure 9. Typical shift in response when an open-ended resonator passes over a subsurface crack in a dielectric.

Figure 10. Typical shift in response when an open-ended resonator is placed over a deep air gap parallel to the sensing surface.

Figure 11. Typical shift in response showing that the resonator senses different backing materials. h = height of teflon cylinder.

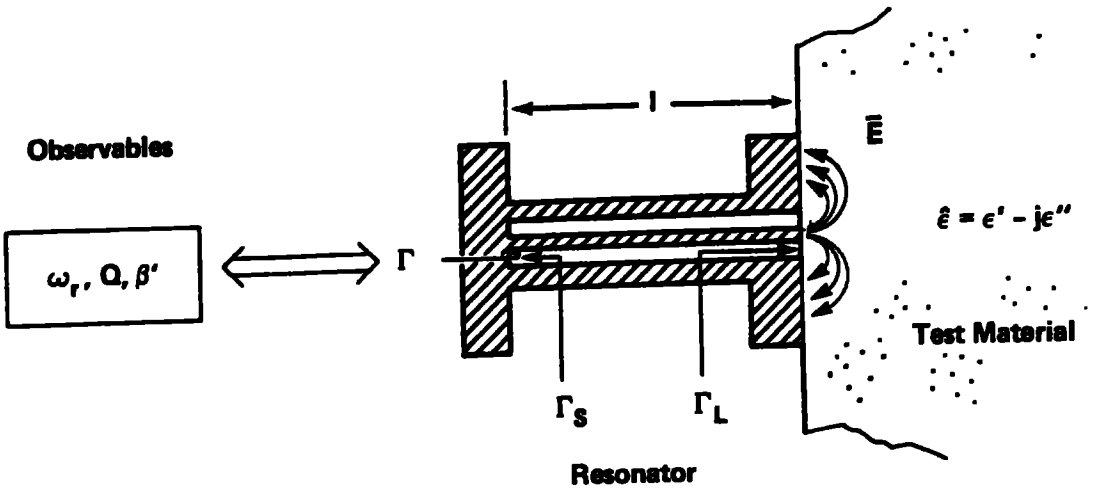

Figure 1

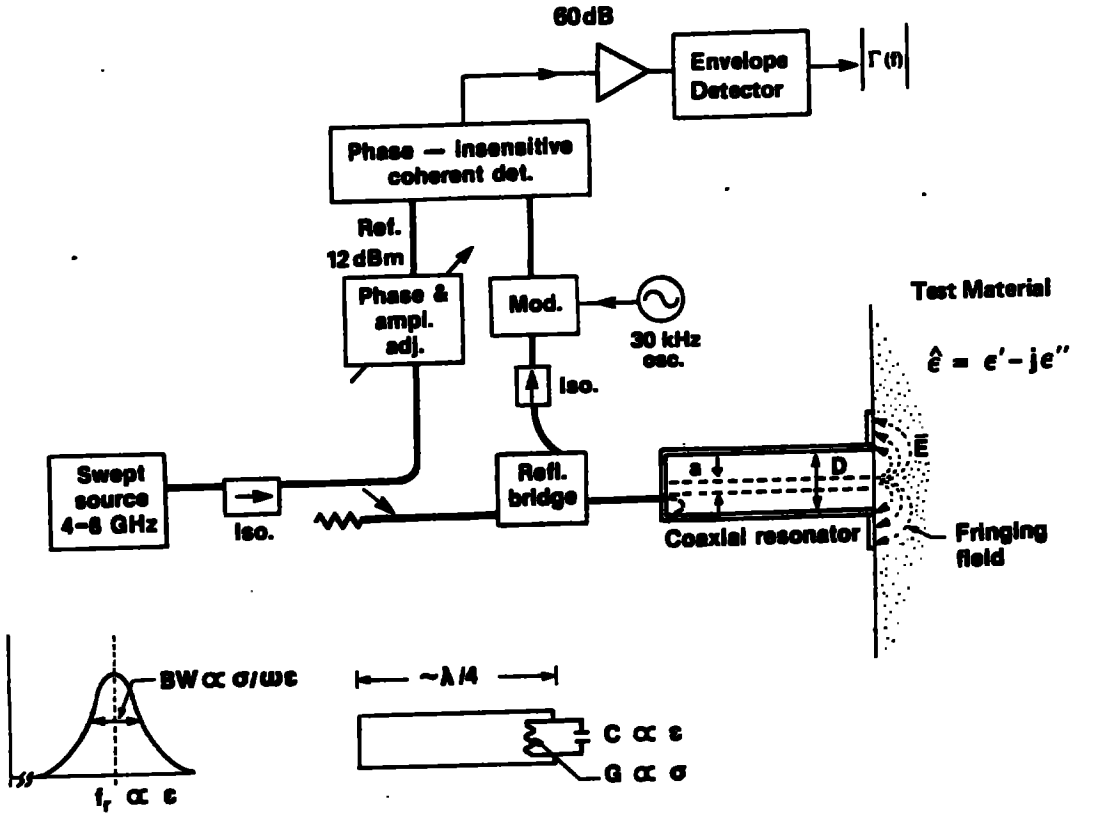

Figure 2

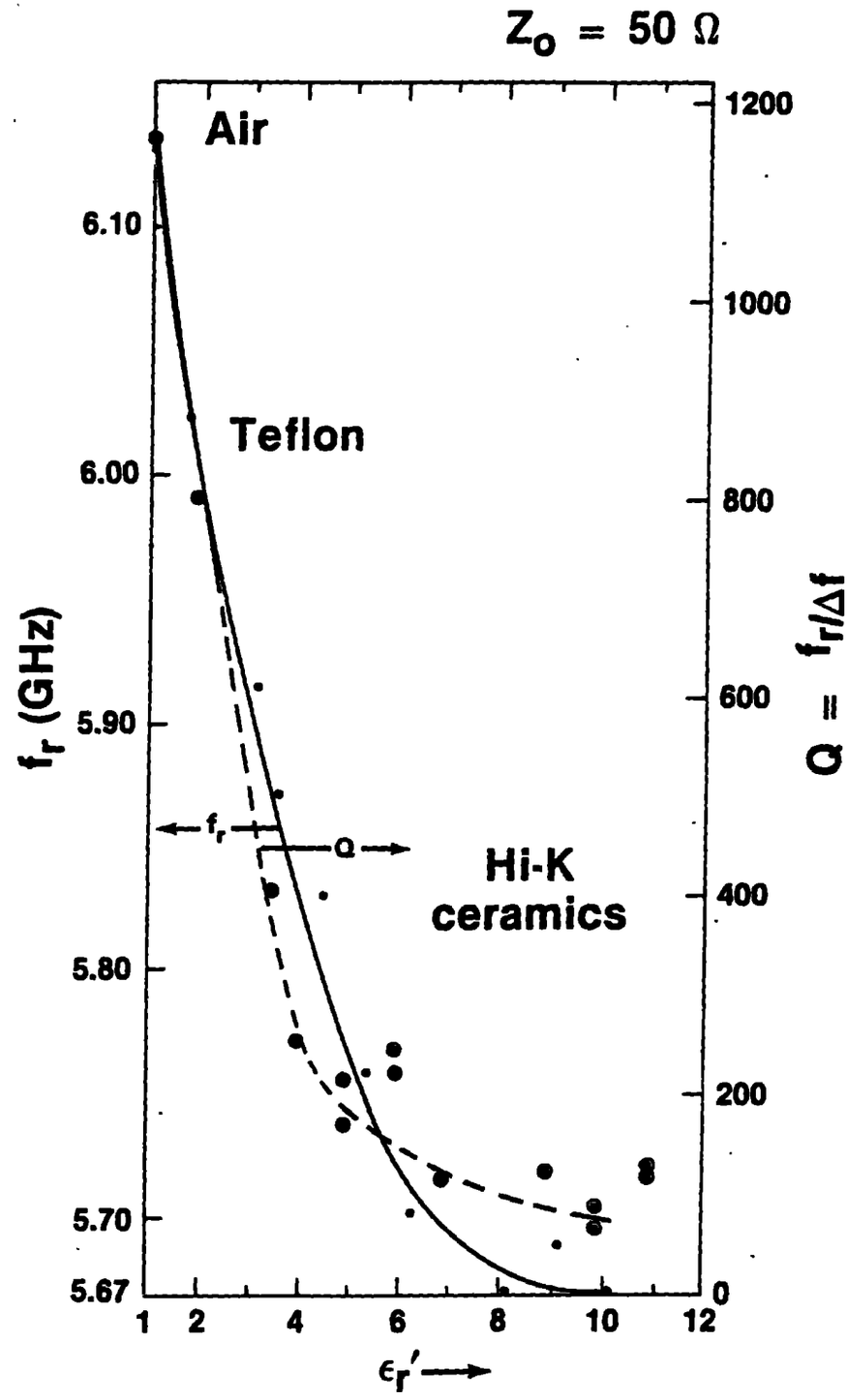
Z_o = 50 Ω
Air
Teflon
Hi-K ceramics
f_r
Q
f_r (GHz)
Q = $f_r/\Delta f$
6.10
6.00
5.90
5.80
5.70
5.67
1200
1000
800
600
400
200
0
1
2
4
6
8
10
12
ϵ_r'

Figure 3

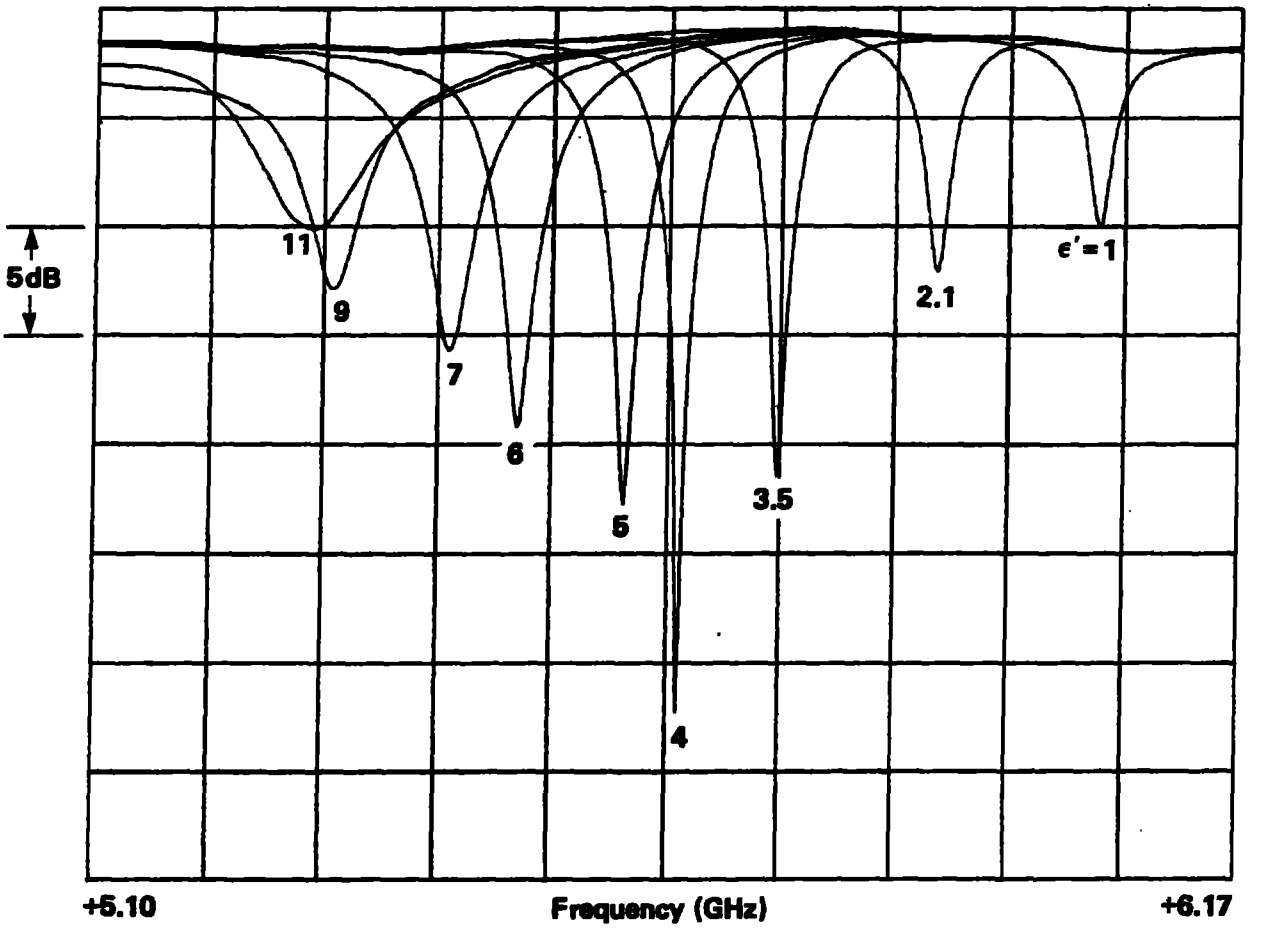

Figure 4

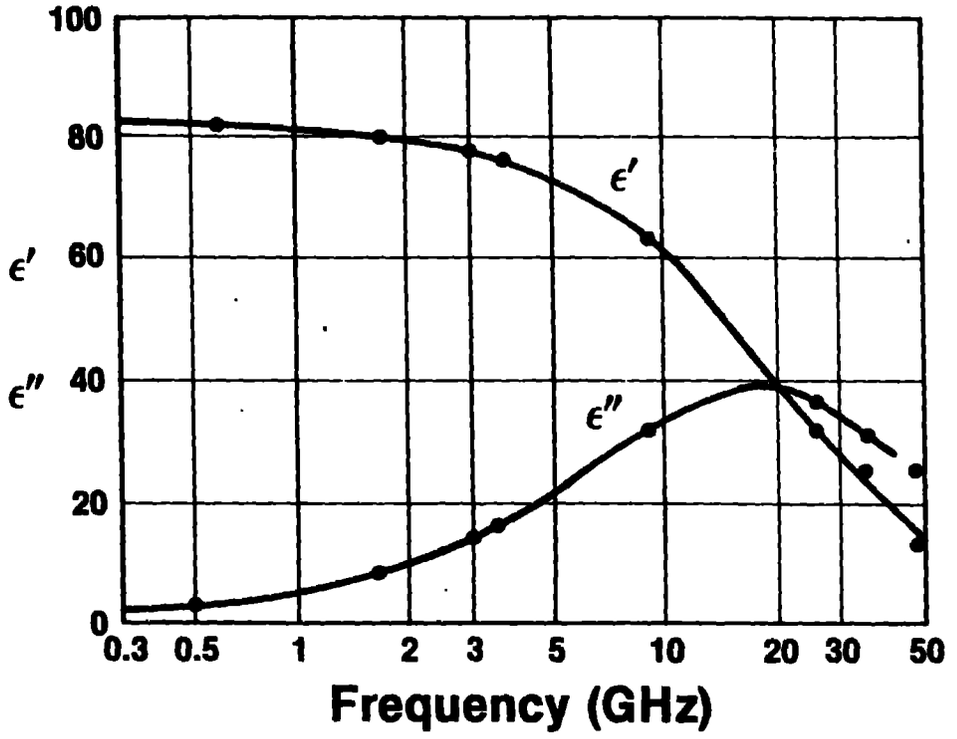

Figure 5

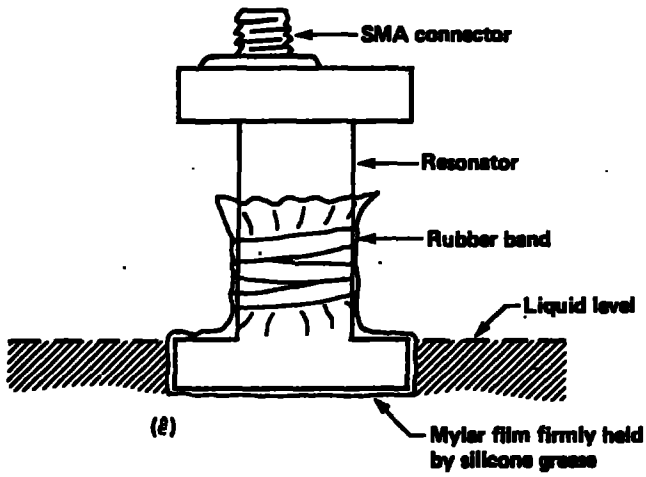

Figure 6

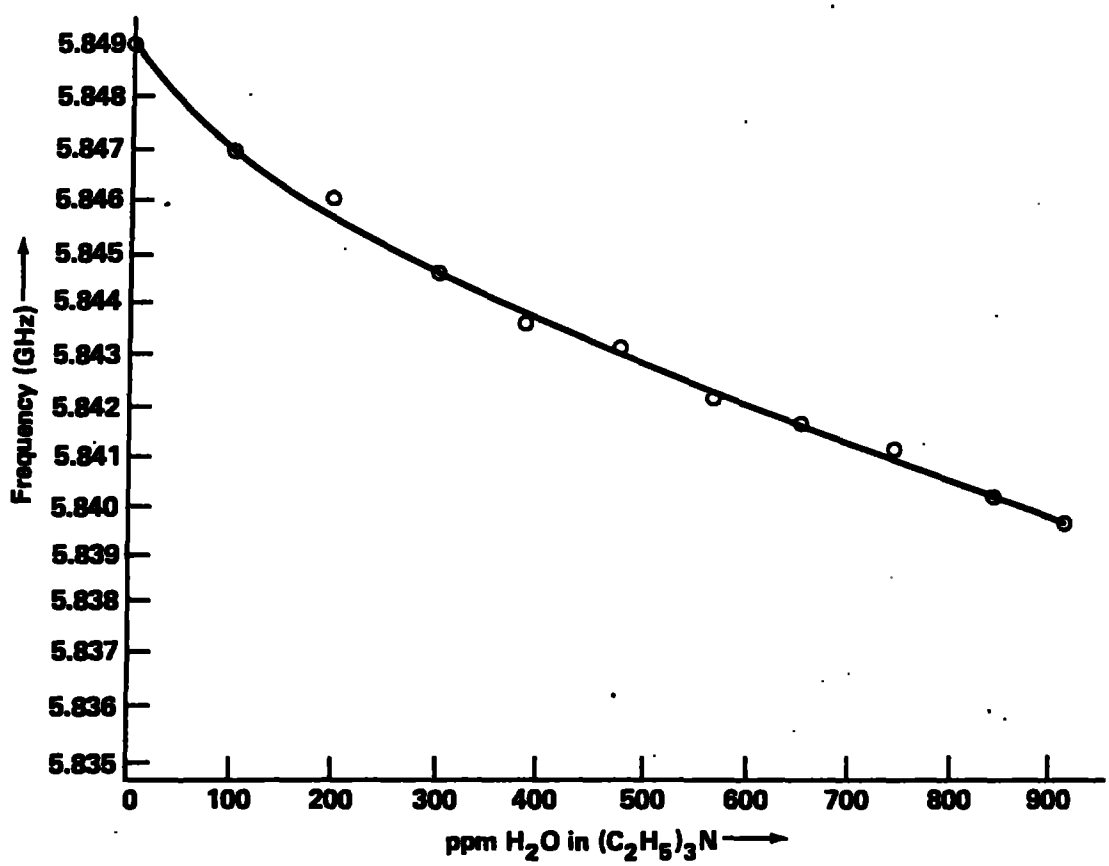

Figure 7

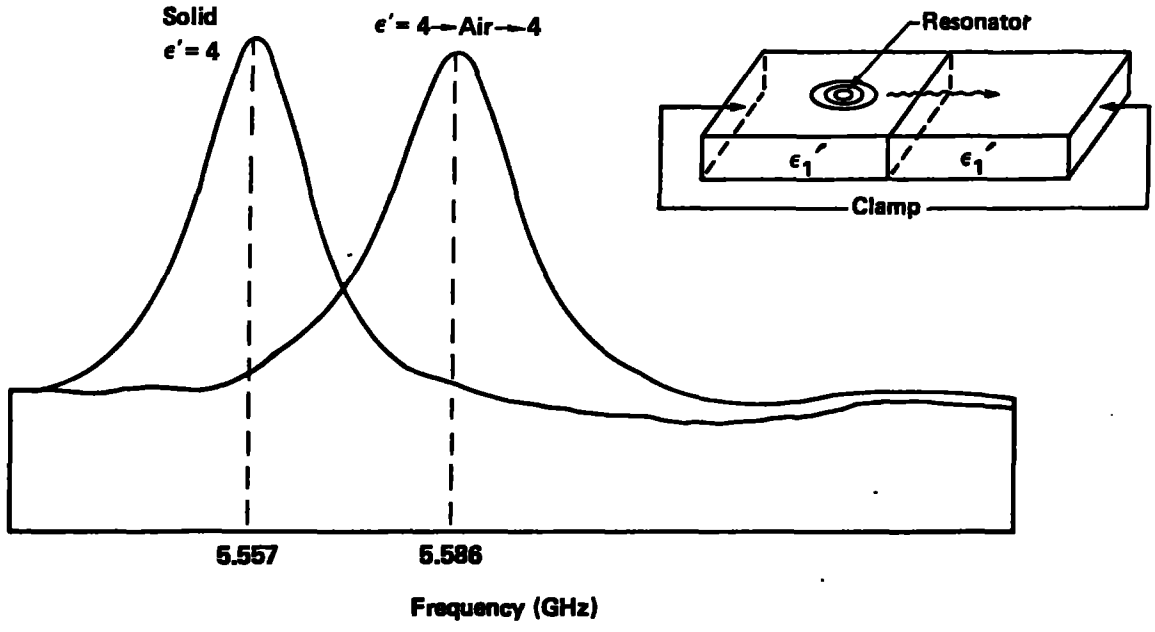

≈ Figure 8

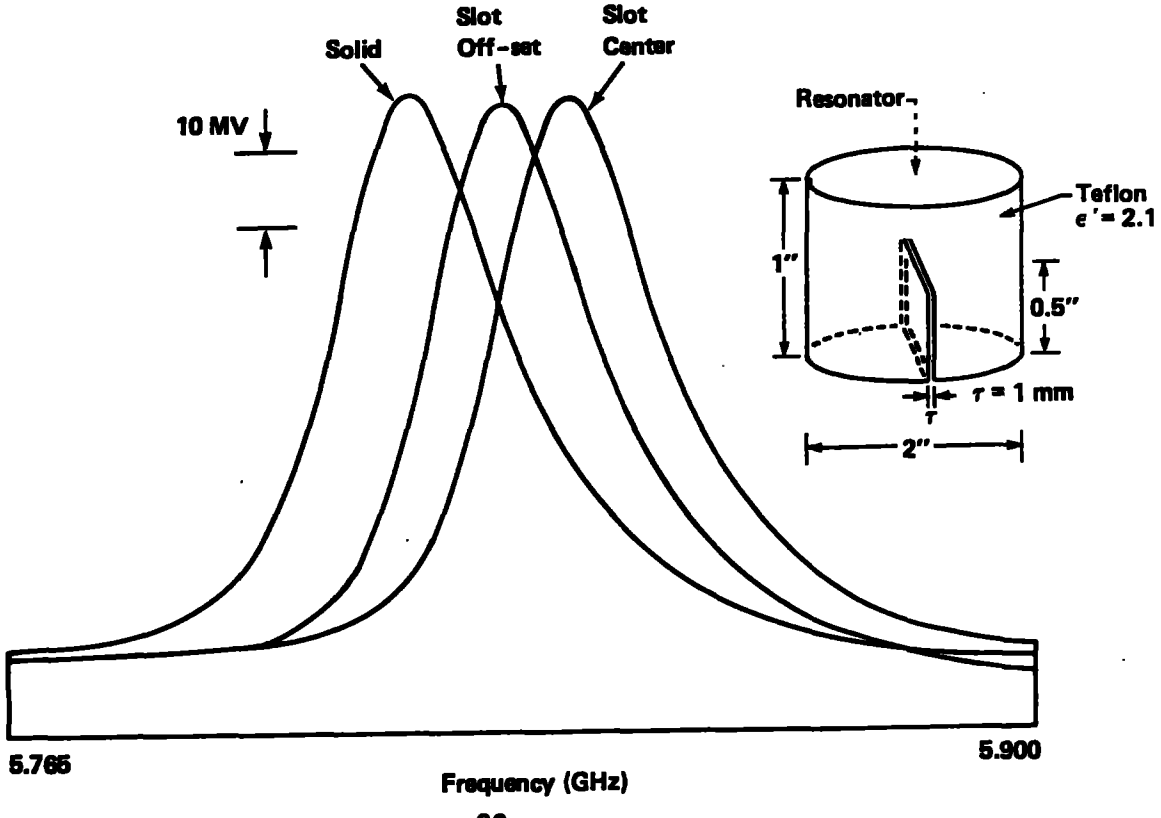

≈ Figure 9

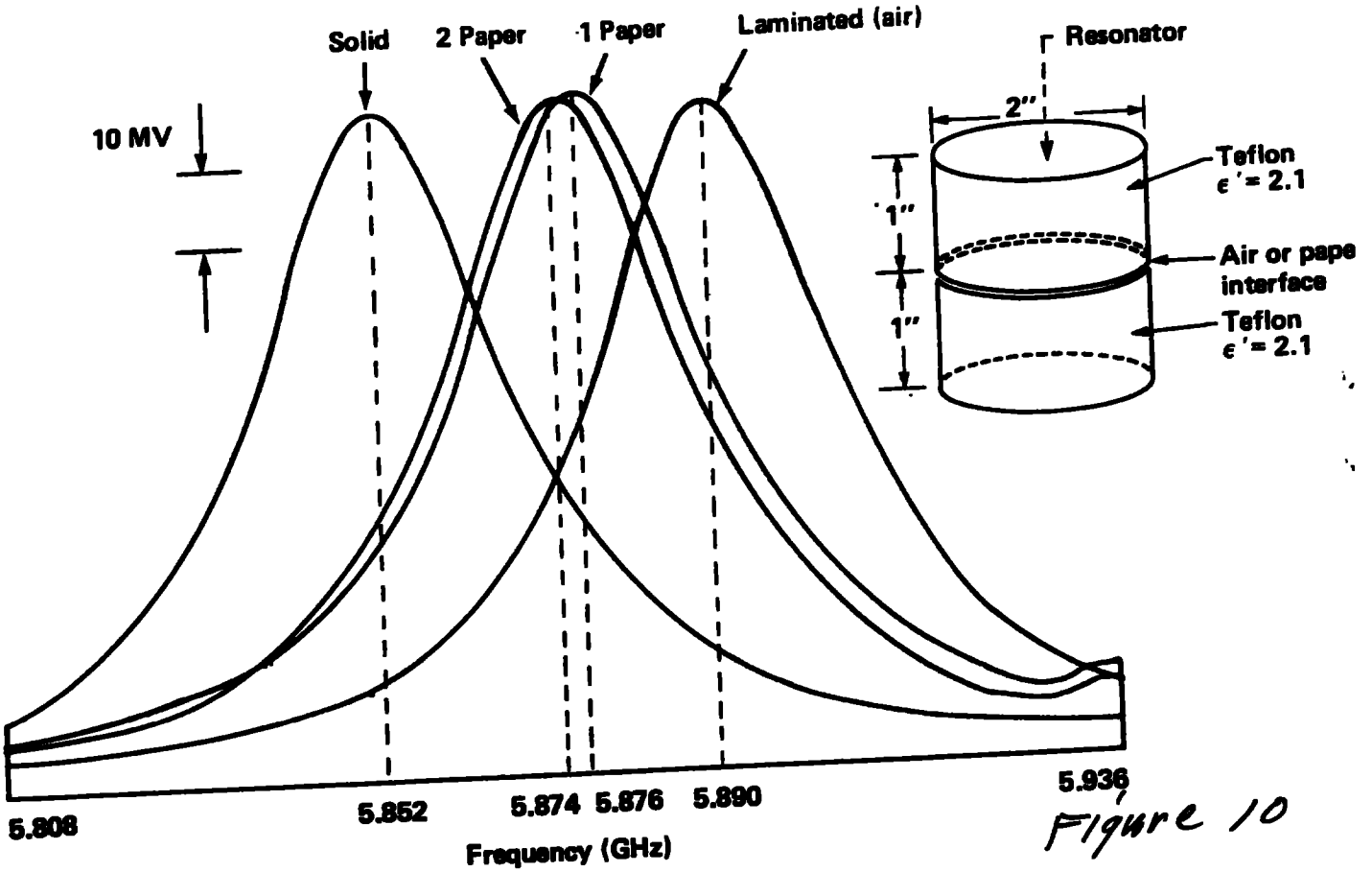

Figure 10

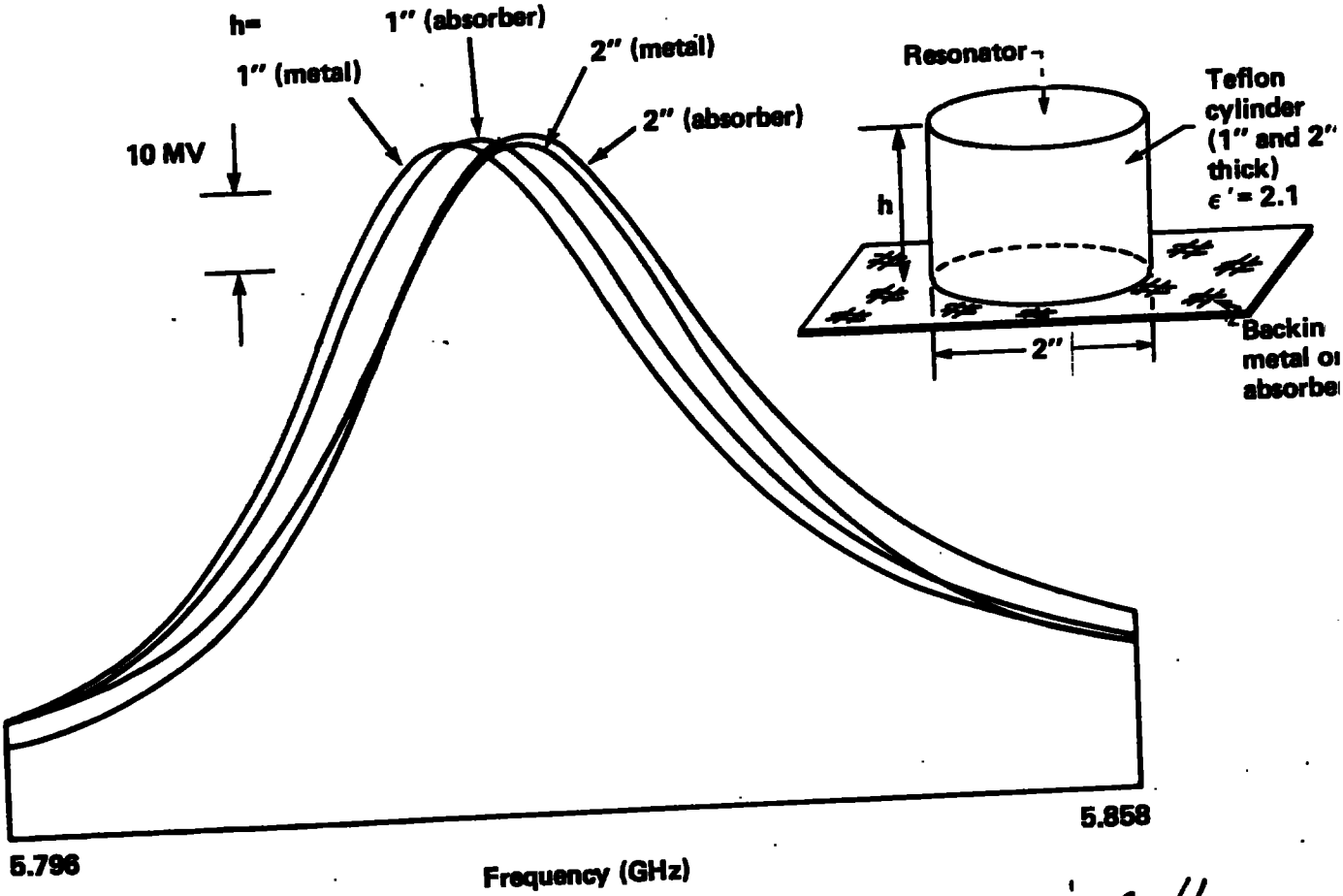

Figure 11